Technical Decision Making with Higher Order Structure Data: Higher Order Structure Characterization During Protein Therapeutic Candidate Screening

YIJIA JIANG, CYNTHIA LI, JENNY LI, JOHN P. GABRIELSON, JIE WEN

Attribute Sciences, Amgen Inc., Thousand Oaks, California 91320

Received 21 October 2014; revised 9 January 2015; accepted 3 February 2015

Published online 26 February 2015 in Wiley Online Library (wileyonlinelibrary.com). DOI 10.1002/jps.24406

ABSTRACT: Protein therapeutics differ considerably from small molecule drugs because of the presence of higher order structure (HOS), post-translational modifications, inherent molecular heterogeneity, and unique stability profiles. At early stages of development, multiple molecular candidates are often produced for the same biological target. In order to select the most promising molecule for further development, studies are carried out to compare and rank order the candidates in terms of their manufacturability, purity, and stability profiles. This note reports a case study on the use of selected HOS characterization methods for candidate selection and the role of HOS data in identifying potential challenges that may be avoided by selecting the optimal molecular entity for continued development. © 2015 Wiley Periodicals, Inc. and the American Pharmacists Association J Pharm Sci 104:1533–1538, 2015

Keywords: protein; candidate selection; higher order structure; biophysical characterization; CD; DSC; DLS; SEC; stability

INTRODUCTION

Higher order structure (HOS) characterization is employed to study the structure–function relationship and stability of proteins.[1,2] Many biophysical techniques including circular dichroism (CD), FTIR, fluorescence spectroscopies, and differential scanning calorimetry (DSC) have been used widely to study protein HOS.[3–10] Changes in the HOS of proteins have been implicated in their decreased stability and potency.[11,12] During protein therapeutics development, a potential product will go through many processing and storage steps (e.g., extreme pH, elevated temperature) exerting stresses that may lead to changes in protein structure. To ensure the selection of the optimal molecule for commercialization, candidate screening is carried out by biopharmaceutical companies.[13–15] Characterization of HOS, along with other analyses, provides enhanced insight into structure and stability, which can often differentiate one candidate from another.

The study reported here is one of a series of case studies arising from an HOS Consortium, which was organized to study how HOS methods and data are currently used in the biopharmaceutical industry to make technical decisions during development of biologics. In this short note, we discuss the use of HOS methods in the context of selecting one protein molecule from two potential candidates that bind to the same biological target, a specific and very relevant industrial application of HOS characterization. We show that HOS methods may be used in concert with other analytical methods to make a technical decision about a candidate's likelihood for success during development.

The degree of rigor required to characterize the chemical and physical structures of therapeutic products changes during the course of development. At early stages of product development, the amount of data and extent of analysis applied to characterize biopharmaceutical products is typically small compared with the data requirement later in development. By the time a product is sufficiently advanced to apply for marketing authorization, it must be comprehensively characterized. Phase appropriate characterization also applies to making decisions during development. Thus, for the purpose of candidate selection, as described in this case study, only a limited amount of HOS data were collected as deemed sufficient to make the decision.

Antibodies X and Y are IgG 2 mAbs against the same target, and they exhibit similar biological activities. The HOSs and relative stabilities of the two molecules were characterized for an initial assessment of manufacturability and overall product quality. The effect of pH on the conformation and thermal stability of the two candidates was assessed at pH 3 and at pH 7 by several biophysical methods including near UV CD, FTIR, fluorescence spectroscopy, and DSC. In addition, the size distribution of each candidate mAb was measured by dynamic light scattering (DLS) because significant differences in self-association of mAbs had been previously observed at pH 2–8 in studies of other antibodies.[16–18] The reversibility of pH-induced changes was analyzed by dialyzing the protein into phosphate-buffered saline (PBS) following 2-h incubation at ambient temperature in pH 3 solution. The storage stability of the molecules at their formulation pH of 5, and a temperature of 37°C, was assessed by size-exclusion HPLC (SE-HPLC). The pH of 3, 5, and 7 were chosen to mimic actual conditions of production and storage.

MATERIALS AND METHODS

Materials

mAbs X and Y were produced at Amgen (Thousand Oaks, California) with purities of at least 99% by SE-HPLC. The decision for lead candidate selection was based on HOS and stability

Correspondence to: Yijia Jiang (Telephone: +805-499-7548; Fax: 805-492-8829; E-mail: yijia3658@gmail.com); Cynthia Li (Telephone: +805-447-1151; Fax: +805-375-6416; E-mail: cynthial@amgen.com)

This article contains supplementary material available from the authors upon request or via the Internet at http://onlinelibrary.wiley.com/.

Journal of Pharmaceutical Sciences, Vol. 104, 1533–1538 (2015)

data collected for both mAbs at protein concentrations ranging from 0.5 to 70 mg/mL depending on the condition and method as detailed here. For the pH study, the two samples (at 10.6 and 18.2 mg/mL, respectively) in 10 mM sodium acetate buffer at pH 5 were diluted to about 0.5 mg/mL in 20 mM sodium citrate, 140 mM NaCl, at pH 3 (C3N) and separately into PBS buffer at pH 7 to about 0.5 mg/mL.

To study the reversibility of HOS changes, samples (2 mL) of each of the antibodies (X and Y), diluted into C3N at 0.5 mg/mL protein concentration, were incubated at room temperature for 2 h, and then dialyzed against 3 L of PBS using dialysis cassettes overnight without further buffer exchange. The dialyzed samples were stored at 4°C until analysis. The changes in buffer conditions and pH were selected to mimic the viral inactivation and neutralization processing steps which the antibodies undergo during purification.

Methods

Near UV CD spectra were obtained on a Jasco J-715 spectropolarimeter (Oklahoma City, Oklahoma) at ambient temperature. Mabs X and Y were each analyzed at a concentration of about 0.5 mg/mL, using cuvettes with a path length of 1 cm (340–240 nm); each spectrum was an average of 10 scans, and a single spectrum of each sample was collected. The spectra are normalized by the protein concentration and reported as mean residue ellipticity.

Spectral similarities of CD spectra were calculated using Thermo Fischer Scientific (Waltham, Massachusetts) OMINC QC compare software. The QC Compare function correlates the spectral features of two spectra in a specified wavelength region to determine the similarity between them. The result is a value between 0% and 100%, which indicates how closely the spectra match each other (100% for identical spectra). Because of the natural variability in the CD technique, as discussed in Reference3, replicate measures of the same sample typically have a similarity of 95% or higher.

Size variant distributions of the candidate samples were determined using a Malvern Zetasizer Nano ZS instrument (Westborough, Massachusetts) at 20°C using a low volume glass cuvette (50 μL). The viscosity (1.0041 cP) and refractive index (1.330) were used for calculating the size distribution of the proteins. All samples were measured at a concentration of about 0.5 mg/mL. Dispersion Technology Software (DTS) v5.03 was used for data collection and analysis. More than 10 runs of 10 s each were performed for each measurement. At least duplicate measurements were performed for each sample. For data processing, general purpose with normal resolution mode was used. The averaged intensity-weighted (*Z*-average) hydrodynamic diameter and polydispersity index (PDI) were reported.

The DSC experiments were performed using a MicroCal VP-Capillary DSC system (GE Healthcare Bio-Sciences, Pittsburgh, Pennsylvania), and data analysis was conducted using MicroCal Origin software version 7. Samples were heated at a rate of 60°C/h with a 15 min pre-scan and a 10 s filtering period. The built-in baseline correction function was used after subtracting the corresponding buffer scan. After baseline correction, the apparent thermal transition midpoints of each sample were determined by the built-in T_m determination function in the software. As with the CD and DLS measurements, the protein concentration was approximately 0.5 mg/mL for all DSC scans.

The final purified mAb X and Y proteins were prepared at 70 mg/mL and pH 5. The antibody samples were vialed and incubated at 37°C for up to 4 weeks, and the stability was assessed by SE-HPLC to monitor the loss of monomer and formation of high-molecular-weight species (HMWS). An Agilent 1100 HPLC system was used to collect the SE-HPLC data. The samples were injected on a Tosoh Bioscience TSK-GEL G3000SW$_{xl}$ column (5 μm, 7.8 × 300 mm^2) and eluted isocratically using a mobile phase of 150 mM sodium phosphate, 300 mM sodium chloride, pH 6.8 at a flow rate of 0.5 mL/min at ambient temperature. Absorbance was measured at 215 nm. The chromatogram was divided into regions representing the protein monomer, HMWS and low-molecular-weight species. The regions were individually integrated, and their respective areas were reported relative to the total area of the three regions.

Although other biochemical and biophysical methods were used in the candidate selection studies, including FTIR and fluorescence spectroscopies, only results from near UV CD, DLS, DSC, and SE-HPLC are reported here, as they were most sensitive to the irreversible changes in conformation and self-association of mAbs X and Y. (FTIR spectra are shown as supplement information.)

RESULTS AND DISCUSSION

Conformation

Circular dichroism spectra in the near UV region can be used to study tertiary structure.[3] The near UV CD spectra of mAbs X and Y in C3N and PBS are shown in Figure 1. The CD spectra of mAbs X and Y at pH 5 were not collected based on our previous experiences on multiple mAbs that show no differences in their CD spectra between pH 5 and 7. Although there may be exceptions, mAbs are generally folded at pH 5–7, and in this case *in vitro* potency data confirmed that the proteins were biologically active, and hence properly folded, at pH 5. Because of the differences in the primary sequences of the two mAbs, their near UV CD spectra differ from each other in both buffers. However, both proteins contain signals at 291–293 and 286–289 nm attributable to tryptophan, fine structure between 270 and 285 nm attributable to tyrosine and tryptophan, and features between 250 and 270 nm attributable to phenylalanine and tyrosine, superimposed on the broad negative disulfide signal from 250 to 280 nm. At pH 3, the spectra of both candidates show a loss in the intensity of the disulfide signal and changes in peak intensity and position at 291–293 and 286–289 nm because of the changes in the tryptophan signal. This indicates that both proteins undergo a significant loss of tertiary structure at pH 3.

In order to compare the spectral changes quantitatively, the overall similarity between a sample spectrum and a control spectrum was calculated.[3,19] The similarity of the near UV CD spectrum of mAb X in C3N compared with its spectrum in PBS is 51%, whereas that of mAb Y in C3N to PBS is 43%. Given the spectral similarity precision of CD measurements from a multisite and instrument study is 5%,[3] the difference in spectral similarity of 51% for mAb X compared with 43% for mAb Y is significant, suggesting that the near UV CD spectral changes are less pronounced for mAb X and hence its tertiary structure is slightly more stable at pH 3 compared with that of mAb Y.

The spectra of both candidates incubated in C3N for 2 h and then dialyzed into PBS are also shown in Figure 1. The

 DOI 10.1002/jps.24406

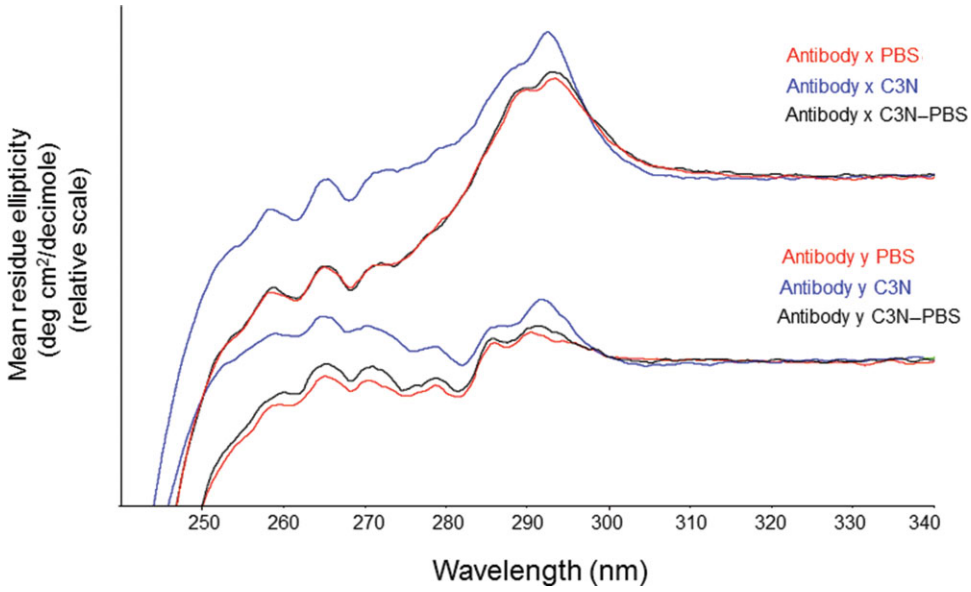

Figure 1. Near UV CD spectra of mAb X and mAb Y at pH 3 (C3N, blue), pH 7 (PBS, red), and pH 7 after pH 3 treatment (C3N–PBS, black).

spectrum of mAb X incubated in C3N for two hours and then dialyzed into PBS is very similar to its spectrum in PBS without low pH exposure, with a spectral similarity greater than 95%. This result suggests that the pH 3-induced changes in the tertiary structure of mAb X are fully reversible after dialysis into PBS. However, the spectrum of mAb Y incubated in C3N for 2 h and then dialyzed into PBS is not comparable to its original spectrum in PBS, with some loss of signal from the disulfides. The spectral similarity of the near UV CD spectra of mAb Y in C3N–PBS compared with PBS is 85%. This indicates that the pH-induced changes in tertiary structure of mAb Y at pH 3 are mostly, but not fully, reversible upon dialysis into PBS. The CD method cannot differentiate whether all mAb Y molecules undergo small changes in their tertiary structure or only a small subpopulation of mAb Y has significantly altered tertiary structure. Nevertheless, if the latter is the case, the presence of a conformational variant can potentially affect the purification yield if the process is developed to remove the misfolded/unfolded species. If the species is not sufficiently removed by the purification process, the conformational variant may adversely affect long-term stability of the product by acting as nucleation sites for further denaturation and aggregation.

Size Distribution

The size variant distributions of the candidates were determined by DLS. DLS measures the time correlation of the intensity of scattered light to determine the diffusion coefficient of molecules and/or particles present in a liquid. Particles with a larger hydrodynamic diameter diffuse more slowly than smaller particles, so the light scattering autocorrelation decay rate of larger particles is longer than that of smaller particles. The *Z*-average hydrodynamic diameter and PDI results from the cumulant fit of the correlation curves of the two candidates at different pH are reported in Table 1. The size distribution by intensity profiles of mAb X and mAb Y at pH 3 and 7 are overlaid in Figures 2 and 3, respectively. MAb X and Y are properly folded with no change in the amount of aggregates at pH values between 5 and 7; therefore, the DLS data at pH 5 were not collected.

Table 1. *Z*-Average and PDI Values of the Candidates

	After Centrifugation			
Sample Name	*Z*-Average (nm)	STDEV (*Z*-Avg) (nm)	PDI	STDEV (PDI)
Antibody X C3N	14.6	0.3	0.27	0.02
Antibody Y C3N	14.6	0.4	0.26	0.03
Antibody X PBS	10.7	0.1	0.04	0.01
Antibody Y PBS	11.7	0.1	0.17	0.01
Antibody X C3N->PBS	13.7	0.1	0.13	0.01
Antibody Y C3N->PBS	18.8	0.1	0.18	0.01

At pH 7 in PBS, both candidates showed similar low *Z*-average diameters (ca. 11–12 nm, consistent with the presence of antibody monomer) and low PDI, indicating both samples were relatively homogeneous. The *Z*-average hydrodynamic diameters and PDIs of the mAbs at pH 3 were significantly higher than those at pH 7 indicating presence of HMWS. The size distribution profiles at pH 3 confirm the presence of large species with hydrodynamic diameters greater than 100 nm. Overall the size distribution and tendency of both candidates to self-associate at pH 3 appear similar. The samples exposed to pH 3 followed by exchange back into PBS at pH 7 have higher *Z*-average diameters and are considerably more heterogeneous than the PBS control samples for both candidates. This observation suggests that larger aggregates that formed at pH 3 were not fully reversible for either candidate. After low pH treatment followed by neutralization, mAb Y had a higher *Z*-average diameter and PDI than mAb X, suggesting that mAb Y aggregates were less reversible than aggregates of mAb X. This correlates with near UV CD data which showed that conformational changes of mAb Y at pH 3 were less reversible than those of mAb X at pH 3, when both samples were exchanged back into PBS at pH 7.

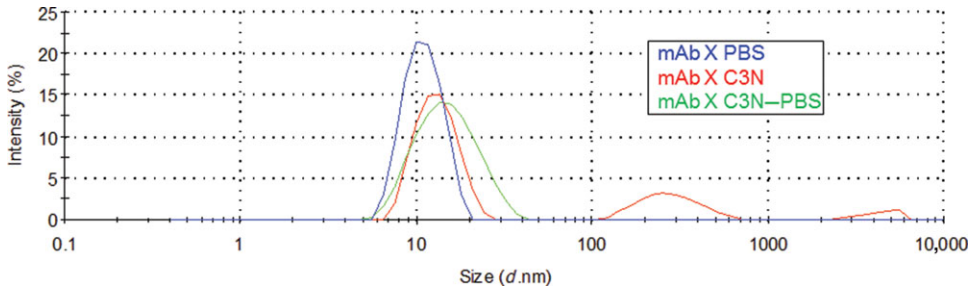

Figure 2. Size distribution by intensity profiles of mAb X at pH 3 (C3N, red), pH 7 (PBS, blue), and pH 7 after pH 3 treatment (C3N–PBS, green).

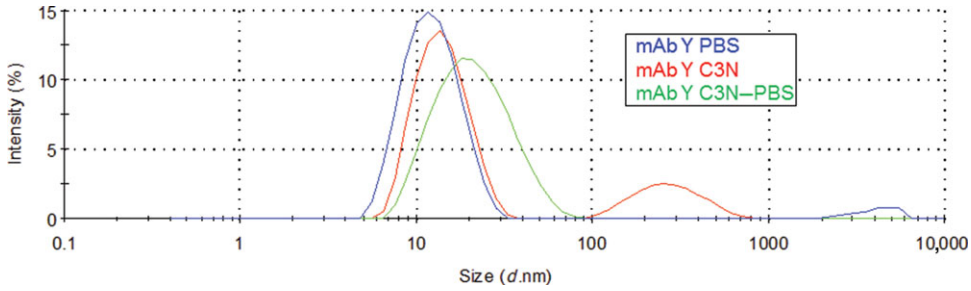

Figure 3. Size distribution by intensity profiles of mAb Y at pH 3 (C3N, red), pH 7 (PBS, blue), and pH 7 after pH 3 treatment (C3N–PBS, green).

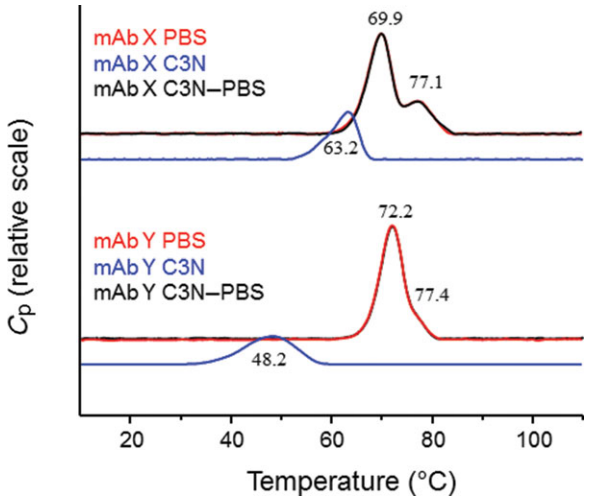

Figure 4. DSC endotherms of mAb X and mAb Y candidate samples. The red scans are mAb X and mAb Y in PBS, the black scans are mAb X and mAb Y in PBS following pH 3 treatment (C3N–PBS), and the blue scans are mAb X and mAb Y in C3N.

Thermal Stability

The thermal stabilities of the candidates were compared by DSC, which can be used to measure the unfolding of protein domains as a function of temperature. The DSC scans of the samples in PBS, C3N, and C3N–PBS are shown in Figure 4. In PBS both candidates exhibited two resolved endothermic transitions: 69.9°C and 77.1°C for mAb X, and 72.2°C and 77.4°C for mAb Y. For both molecules, the first transition corresponded to the unfolding of the constant heavy chain C_H2 and the fragment antigen binding (Fab) domains, and the second transition corresponded to the unfolding of the C_H3 domain. MAb Y was slightly more thermally stable than mAb X in PBS, as all of the mAb Y domains remained folded at the onset of unfolding for mAb X (approximately 65°C).

At pH 3 in C3N, there was only one relatively weak endothermic transition for both candidates, suggesting that the samples were partially unfolded at the starting temperature, due to the low pH. The thermal stability of mAbs is affected by both pH and buffer excipients (e.g., sugars and salts) and usually decreases when the solution pH decreases.[20] The relative ranking between similar mAb molecules typically remains the same (i.e., the same candidate is more stable at higher and lower pH). In this case, the thermal transition temperatures and enthalpies of unfolding of both candidates in C3N were markedly lower than those in PBS, as expected. However, mAb X (T_m of 63.2°C) showed better thermal stability than mAb Y (T_m of 48.2°C) in C3N, even though mAb Y was more thermally stable at neutral pH (mAb X: 69.9°C and 77.1°C and mAb Y: 72.2°C and 77.4°C). Although this result is atypical, it is consistent with the near UV CD data, which showed that mAb X retained more tertiary structure at pH 3. Changes in the thermal stability of the two candidates induced by pH 3 treatment appeared to be fully reversible following dialysis into PBS. Overall, the DSC results indicate that both proteins are very stable at neutral pH, and the thermal stability of mAb Y is higher than that of mAb X in PBS, but lower than that of mAb X in C3N.

Storage Stability

The stability of the candidates at pH 5 after storage at 37°C for up to 4 weeks was assessed by SE-HPLC (Fig. 5). Based on the loss of main peak (monomer) and the corresponding increase in the percentage of HMWS, mAb Y exhibited better storage stability than mAb X at the elevated temperature. This result is consistent with the higher thermal transition temperatures of mAb Y compared with mAb X when folded at neutral pH.

DOI 10.1002/jps.24406

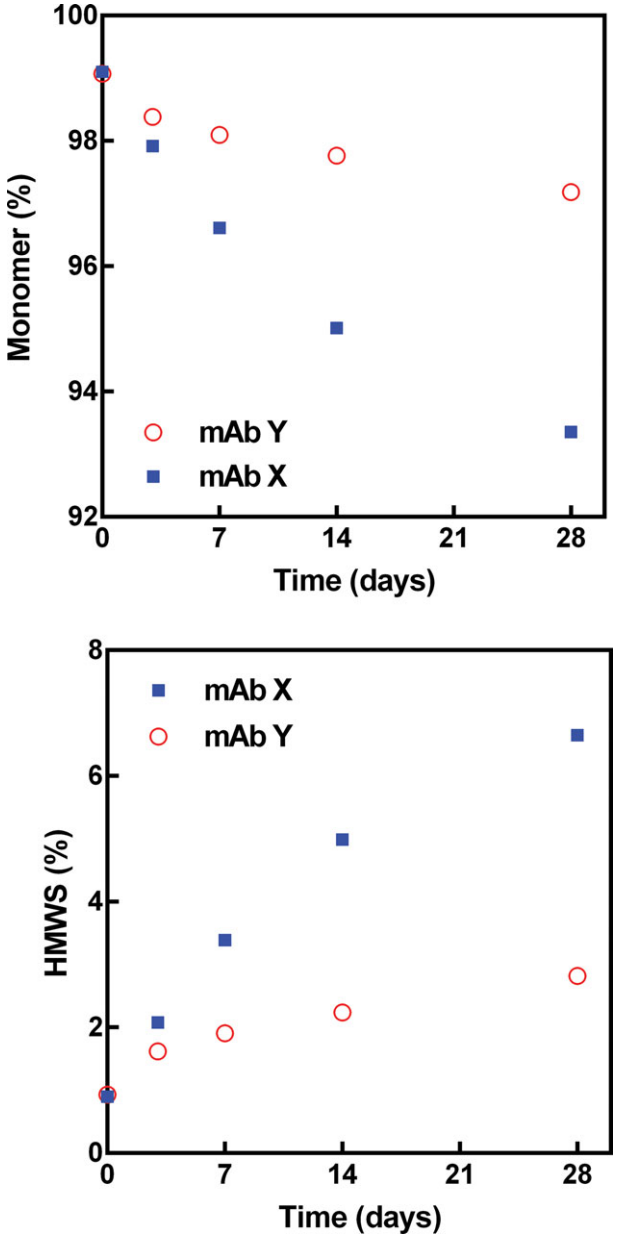

Figure 5. SE-HPLC results of mAb X and mAb Y after storage at 37°C for up to 4 weeks. The results are expressed as main peak (monomer) and high-molecular weight species, both as a percentage of the total integrated area of the chromatogram.

Similar correlations have been observed for other antibodies; lower thermal and conformational stability is generally well correlated with poor expression, decreased storage stability, and increased aggregation levels,[20,21] although there are exceptions to this correlation.[22] Although it is not always appropriate to extrapolate short duration stability results at 37°C to longer term stability at 4°C, in many cases a rank ordering of the stability of multiple molecules at an elevated temperature is valuable when product development timelines require a decision to be made before the results of a longer duration study are available (as was the case here). Longer duration stability studies must still be conducted at the recommended storage condition to confirm stability.

Technical Decision Making

Making a decision to advance one candidate and halt development of another is not always straightforward. As shown in Table 2, both mAbs had reasons to be selected, and the HOS data aided in the decision but was not central to it. Conformational changes and protein self-association were observed for both candidates at pH 3. CD and DSC data showed that mAb Y underwent more structural changes at pH 3 than mAb X. Thermal stability changes induced at pH 3 were fully reversible for both mAbs, although tertiary structural changes appeared to be at least partially irreversible for mAb Y. Compared with mAb X, mAb Y showed better thermal stability at neutral pH and storage stability at 37°C in its formulation buffer at pH 5. Taken together, the results suggest that there are different driving forces for process stability (robustness to pH changes) and storage stability (impact of elevated temperature).

Even though mAb Y was less stable at pH 3 as indicated by CD, DSC and DLS, process clearance studies demonstrated that the downstream purification process was effective in clearing the conformational variant (data not shown) and irreversibly aggregated species (SE-HPLC data at time zero, Fig. 5). Because folded mAb Y had higher thermal stability in PBS at pH 7 and better stability at pH 5 during storage at 37°C, this candidate was recommended to proceed for further development. Because of the irreversibility of both tertiary structure and self-association in PBS that was observed after low pH incubation, the recommendation to advance mAb Y was accompanied by a recommendation to develop the purification process to minimize exposure of mAb Y to pH 3. Minimizing the amount of irreversible aggregate and conformational variant produced by the process will ultimately increase the process yield.

Table 2. Summary of Factors Impacting the Decision to Select mAb Y Instead of mAb X

Factor	mAb X	mAb Y
Tertiary structure	Conformational changes at pH 3; Fully reversible (pH 3 to 7)	Conformational changes at pH 3; Partially irreversible (pH 3 to 7)
Self-association	Aggregation at pH 3; Mostly reversible (pH 3 to 7)	Aggregation at pH 3; Partially irreversible (pH 3 to 7)
Thermal stability	High thermal stability at pH 7; Remaining structure at pH 3 has reduced thermal stability (higher than mAb Y); Fully reversible (pH 3 to 7)	High thermal stability at pH 7 (higher than mAb X); Remaining structure at pH 3 has reduced thermal stability; Fully reversible (pH 3 to 7)
Storage stability	Large increase in HMWS during 4 week storage at 37°C	Small increase in HMWS during 4 week storage at 37°C

CONCLUSIONS

During protein therapeutics development, to select the best candidate for further development, many factors need to be taken into consideration including bioactivity, safety, product quality, and stability. This case study highlights the use of selected biophysical methods to assess protein HOS, and changes in HOS induced by pH changes, ultimately to assist in selecting the optimal candidate for continued development. In this case, the HOS data provided important information about processing conditions, specifically the impact of pH changes during purification, and demonstrated the need for process clearance studies to ensure the conformational variant produced by low pH exposure could be effectively removed from the finished product.

REFERENCES

1. Allewell NM, Narhi LO, Rayment I. 2013. Structural physical and chemical principles. In Molecular biophysics for the life science; Allewell NM, Narhi LO, Rayment I, Eds. New York: Springer, pp 17–30.

2. Alavattam S, Demeule B, Liu J, Yadav S, Cromwell M, Shire SJ. 2013. Biophysical analysis in support of development of protein pharmaceuticals. In Biophysics for therapeutic protein development; Narhi LO, Ed. New York: Springer, pp 173–204.

3. Li C, Nguyen X, Narhi L, Chemmalil L, Towers E, Muzammil S, Gabrielson J, Jiang Y. 2011. Applications of circular dichroism for structural analysis of proteins: Qualification of near- and far-UV CD for protein higher order structural analysis. J Pharm Sci 100:4642–4654.

4. Pelton JT, Mclean LR. 2000. Spectroscopic methods for analysis of protein secondary structure. Anal Biochem 277:167–176.

5. Jiang Y, Li C, Nguyen X, Muzammil S, Towers E, Gabrielson J, Narhi L. 2011. Qualification of FTIR spectroscopic method for protein secondary structural analysis. J Pharm Sci 100:4631–4641.

6. Lakowicz JR. 1982. Principles of fluorescence spectroscopy. New York: Plenum Press

7. Eftink MR. 1994. The use of fluorescence methods to monitor unfolding transitions in proteins. Biophys J 66:482–501.

8. Cooper A, Nutley MA, Wadood A. 2000. Differential scanning microcalorimetry. In Protein–ligand interactions: Hydrodynamics and calorimetry; Harding SE, Chowdhry BZ, Eds. Oxford, New York: Oxford University Press, pp 287–318.

9. Privalov PL. 1982. Stability of proteins: Proteins which do not present a single cooperative system. In Advances in protein chemistry, Anfinsen CB, Edsall JT, Richards FM, Eds. Vol. 35. New York: Academic Press, pp 1–101.

10. Remmele RL, Nightlinger NS, Srinivasan S, Gombotz, WR. 1998. Interleukin-1 receptor (IL-1R) liquid formulation development using differential scanning calorimetry. Pharm Res 15:200–208.

11. Chi EY, Krishnan S, Randolph TW, Carpenter JF. 2003. Physical Stability of Proteins in aqueous solution: Mechanism and driving forces in nonnative protein aggregation. Pharm Res 20(9):1325–1336.

12. Arthur KK, Dinh, NN, Gabrielson, JP. 2015. Technical decision-making with higher order structure data: Utilization of differential scanning calorimetry to elucidate critical protein structural changes resulting from oxidation. J Pharm Sci DOI 10.1002/jps.24313.

13. Narhi LO, Jiang Y, Deshpande R, Kang S, Shultz J. 2010. Approaches to control protein aggregation during bulk production. In Aggregation of therapeutic proteins; Wang W, Roberts CJ, Eds. New Jersey: John Wiley and Sons, pp 257–268.

14. Satish H, Angell N, Lowe D, Shah A, Bishop S. 2013. Application of biophysics to the early developability assessment of therapeutic candidates and its application to enhance developability properties. In Biophysics for therapeutic protein development; Narhi LO, Ed. New York: Springer, pp 127–146.

15. Ramachander R, Rathore N. 2013. Molecule and manufacturability assessment leading to robust commercial formulation for therapeutic proteins. In Sterile product development; Kolhe P, Shah M, Rathore N, Eds. New York: Springer, pp 33–45.

16. Arnoldus WP, Norde VW. 2000. The thermal stability of immunoglobulin: Unfolding and aggregation of a multi-domain protein. Biophys J 78:394–404.

17. Paul M, Vieillard V, Jaccoulet E, Astier A. 2012. Long-term stability of diluted solutions of the monoclonal antibody rituximab. Int J Pharm 436:282–290.

18. Bhambhani AL, Kissmann JM, Joshi SB, Volkin DB, Kashi RS, Middaugh CR. 2012. Formulation design and high-throughput excipient selection based on structural integrity and conformational stability of dilute and highly concentrated IgG1 monoclonal antibody solutions. J Pharm Sci 101:1120–35.

19. Teska B, Li C, Winn B, Arthur K, Jiang Y, Gabrielson J. 2013. Comparison of quantitative spectral similarity analysis methods for protein higher order structure confirmation. Anal Biochem 434:153–165.

20. Wen J, Jiang Y, Narhi L, Hymes K, Gong K. 2007. Correlation between thermal stability and protein stability. In Proceedings of the 2007 current trends in microcalorimetry conference; Reese E, Spotts S, Eds. Northampton, Massachusetts: Micro-Cal LLC, pp 93–108.

21. Garber E, Demarest S. 2007. A broad range of Fab stabilities within a host of therapeutic IgGs. Biochem Biophys Res Commun 355:751–757.

22. Gruia F, Bee J. 2015. Technical decision-making with higher order structure data: Impact of a formulation change on the higher order structure and stability of a monoclonal antibody. J Pharm Sci DOI 10.1002/jps.24158.